Measuring the Modulus of Soft Polymer Networks via a Buckling-Based Metrology

ARTICLE *in* MACROMOLECULES · MAY 2006

Impact Factor: 5.8 · DOI: 10.1021/ma060266b

5 AUTHORS, INCLUDING:

Sheng Lin-Gibson
National Institute of Standards and Technolo…
86 PUBLICATIONS **1,514** CITATIONS
SEE PROFILE

Christopher M Stafford
National Institute of Standards and Technolo…
119 PUBLICATIONS **3,814** CITATIONS
SEE PROFILE

Measuring the Modulus of Soft Polymer Networks via a Buckling-Based Metrology

Elizabeth A. Wilder,† Shu Guo,‡ Sheng Lin-Gibson, Michael J. Fasolka, and Christopher M. Stafford*

Polymers Division, National Institute of Standards and Technology, Gaithersburg, Maryland 20899

Received February 3, 2006; Revised Manuscript Received April 10, 2006

ABSTRACT: We present a new method for measuring the modulus of soft polymer networks ($E < 10$ MPa). This metrology utilizes compression-induced buckling of a sensor film applied to the surface of the specimen, where the periodic buckling wavelength, assessed rapidly by laser light diffraction or optical microscopy, yields the modulus of the network specimen. To guide the development of this new technique, we use classical mechanical analysis to calculate the sensitivity of the critical strain and resulting wavelength of the buckling instability to the modulus and thickness of the sensor film as well as the modulus of the soft material being probed. Experimental validation of our technique employed a series of model cross-linked poly(dimethylsiloxane) elastomers. To further demonstrate the versatility of this method, we measure the moduli of a set of pertinent biomaterials, i.e., cross-linked 2-hydroxyethyl methacrylate (HEMA) hydrogels. Using a hydrogel substrate possessing a gradient in the cross-link density, we also show how this metrology can be used to map spatial differences and heterogeneity in modulus within a specimen.

Introduction

Soft polymers, such as elastomers, gels, and hydrogels, are an important class of materials with applications in a wide range of technologies including adhesives, drug delivery, cell scaffolds, solid electrolytes, and separation media. In these applications, a key metric in the evaluation of soft polymeric systems is the elastic modulus and thus the mechanical behavior of such materials. While the elastic modulus is primarily a measure of stiffness, it is also related to a variety of other performance factors including adhesion, swelling behavior, and the propensity for cell proliferation and growth in biomaterials.[1−3] For many applications, traditional measurement techniques including common tensile and compression tests are typically used to assess elastic modulus of these systems provided that specimens of adequate size and shape (e.g., "dog bone" or cylindrical samples) can be prepared.

Increasingly, however, the development of new soft materials demands rapid, more versatile measurement methods that can accelerate and enhance the engineering of these materials for specific applications.[4,5] For example, the preparation of large specimens can be untenable when the synthesis of new materials is expensive and time-consuming or results in low yield, as is often the case for biomaterials[6−9] and specialty elastomers.[10−12] Moreover, for many applications it is desired that modulus measurements be conducted on specimens that assume a specific geometry or under specific conditions. Here, an illustrative example is found in the testing of contact lens materials, where examination of prototype lens devices in a hydrated state is necessary to judge performance. Such in situ measurements can be particularly challenging if the specimen size is necessarily small (as noted above) or if determination of spatial variations in modulus is desired. Finally, the discovery and optimization of soft materials would be advanced by "high-throughput" methods that enable rapid, automated measurements of the modulus of many specimen formulations. Again, traditional tensile and compression tests are inadequate since they are based on a slow "one at a time" measurement paradigm. In these respects, local probe techniques, in particular nanoindentation, are attractive. Indeed, for hard materials such as ceramics, metals, and certain glassy polymers, nanoindentation can address some of the issues discussed above.[13,14] However, nanoindentation measurements are generally unproven for the modulus range exhibited by soft materials.[15]

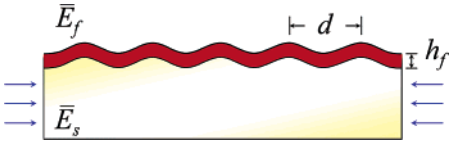

Figure 1. Schematic of buckling of a thin stiff plate (red) on an elastic foundation induced by a compressive strain applied to the system. Typical sample dimensions: sensor film thickness (h_f): 100 nm; substrate thickness: 1 mm; surface area of sensor film and substrate range from 1 to 20 cm^2.

In response to these metrology challenges, this paper introduces a measurement platform for assessing the elastic modulus of soft polymer networks and gels. The current method adapts a metrology developed previously for measuring the elastic modulus of thin films and coatings, which leverages an elastic buckling instability that occurs upon compression of a stiff upper film supported by a soft elastic substrate.[16,17] In contrast to our previous work, we outline means by which this metrology can be "reversed" to focus on measuring the moduli of soft material substrates. As will be seen below, our technique accommodates the challenges of small specimens, in situ evaluation, spatial modulus imaging, and high-throughput measurement capabilities. This metrology is also simple and inexpensive to implement without the need for investment in intricate and often delicate instrumentation, thus lowering the barrier for broad and widespread application of this measurement technique.

Background on Buckling Mechanics. As discussed above, our measurement platform utilizes a buckling instability that occurs upon compression of a bilayer laminate consisting of a relatively stiff thin plate mounted on an elastic foundation, which is illustrated in Figure 1. The mechanics of such systems is described well by analytical expressions in the literature.[18−21]

† Present address: Corporate Research Division, The Procter and Gamble Company, Cincinnati, OH 45253.

‡ Present address: The Dow Chemical Company, Freeport, TX 77541.

* Corresponding author: Fax +1 (301) 975-4924; e-mail chris.stafford@nist.gov.

10.1021/ma060266b
Published on Web 05/18/2006 PAGE EST: 5.6

To outline the measurement strategy, we provide here the equations pertinent to this metrology. In short, to minimize the total strain energy of the system, the compressed laminate undergoes buckling to form a highly periodic, sinusoidal surface. The periodicity of the buckling pattern is primarily dependent on the modulus ratio between the film and substrate as well as the thickness of the upper film:

$$d = 2\pi h_f \left(\frac{3\bar{E}_f}{\bar{E}_s}\right)^{1/3} \quad (1)$$

where d is the wavelength of the instability, h_f is the thickness of the film, $\bar{E} = E/(1 - \nu^2)$ is the plane-strain modulus, and ν is Poisson's ratio. The subscripts "f" and "s" denote film and substrate, respectively. In our validation studies,[16] the modulus of the upper film was the unknown to be measured (all else being known or constant):

$$\bar{E}_f = 3\bar{E}_s \left(\frac{d}{2\pi h_f}\right)^3 \quad (2)$$

In this study, we "reverse" the experimental design by using a sensor film of known modulus and thickness, thus rearranging eq 2 as follows:

$$\bar{E}_s = \frac{\bar{E}_f}{3}\left(\frac{d}{2\pi h_f}\right)^{-3} \quad (3)$$

Thus, we are able to determine the modulus of the soft elastic substrate, $\bar{E}_s$. It should be noted that in the analytical solution the substrate is treated as semi-infinite half-space, and therefore the thickness of the substrate does not factor into eqs 2 and 3. However, the decay of the stress normal to the surface (into the substrate) is given by[19]

$$\sigma_z(z) \sim \exp\left(-\frac{2\pi}{d} z\right) \sin\left(\frac{2\pi}{d} x\right) \quad (4)$$

Consequently, the depth (or thickness) to which the buckling instability is sensitive to the elastic modulus of the substrate is on the order of the wavelength of the instability, d. Accordingly, different wavelengths would probe different depths into the substrate.

Experimental Section[22]

Substrate Preparation. Poly(dimethylsiloxane) (PDMS) (Sylgard 184, Dow Chemical Co., Midland, MI) was used in the model study. Compositions of 5:1, 10:1, 15:1, 20:1, and 25:1 mass ratios of base monomer to curing agent were hand-mixed and cast onto glass plates. The mixtures were left at room temperature to allow trapped air bubbles to escape and then cured at 70 °C for 2 h. After cooling, the PDMS was cut into 75 mm × 25 mm specimens.

Model hydrogel systems were fabricated by mixing 2-hydroxyethyl methacrylate (HEMA) (Esstech, Essington, PA) with a cross-linker, diethylene glycol dimethacrylate (Esstech), at various mass fractions. The systems were further prepared for photopolymerization by adding 1 mass % Irgacure 819 (Ciba Specialty Chemical Corp., Tarrytown, NY) as an initiator. The resin mixture was then syringed into a "sandwich" mold consisting of two glass slides and a PDMS spacer ($t \approx 3$ mm). To facilitate the removal of polymerized HEMA, the glass slides were pretreated with octadecyltrimethoxysilane to render the surfaces hydrophobic. The mixture was polymerized with visible light ($\lambda = 470$ nm) for a total of 3 min using a Triad 2000 visible light curing unit (Dentsply, York, PA). After curing, the poly(HEMA) gels were soaked in distilled water for a minimum of 72 h to ensure equilibrium swelling. The hydrogels were then cut or stamped into the appropriate test geometries. Specimens were cut after curing and soaking to avoid dimensional changes due to polymerization shrinkage and subsequent swelling.

Gradient Substrates. PDMS gradient samples with varying curing agent composition were prepared by individually casting the separate specimens within the same sample. Initially, a 10:1 casting was cured for 1 h. After curing, a small cutout was removed from the 10:1 sample and replaced with an uncured 15:1 casting. This altered sample was then cured for an additional 1 h, and the cycle was repeated for the 20:1 casting. After the three individual castings were complete, a 10:1 mixture was cast over the back of the entire sample to ensure a uniform thickness over the entire gradient sample in order to compensate for any under- or overfilling of the cutouts.

The poly(HEMA) hydrogel composition gradient was prepared in a similar manner. A strip of HEMA monomers of a given composition was syringed into a rectangular mold and photopolymerized. Then HEMA monomers of a different cross-linker composition were syringed over the existing strip and photopolymerized. This sequential curing process was repeated to generate the discrete poly(HEMA) gradient sample. The gradient gel consisted of strips of poly(HEMA) possessing cross-linker ratios of 0.5, 1, 2, 4, and 8 mass %.

Polystyrene (PS) Sensor Film Preparation. Solutions of 2% PS ($E_f = 3.5$ GPa) in toluene were spin-coated onto clean, UV-ozone treated silicon wafers at 2000 rpm for 15 s. The thickness of the films, as determined by interferometry, was 88 ± 2 nm, unless otherwise noted. For each specimen the thickness was determined by taking the average of at least 16 measurements across the sample.

Film/Substrate Assembly and Characterization of Modulus. The PS/PDMS specimens were prepared as previously described.[16] Briefly, a PDMS substrate was loaded onto a custom-built strain stage and strained (in tension) to 2.5%. The sensor film of known thickness was transferred to the surface of the prestrained PDMS. Release of the applied strain results in a net compressive strain on the bilayer specimen; the strain was released slowly until buckling occurred. For the gradient samples, PS films were transferred to the specimen in the same manner, although a slightly higher strain (≈3%) was used in order to ensure that buckling was seen across all compositions. In order for buckling to occur, the adhesion of the sensor film to the substrate must be sufficient to transfer stress across the substrate/film interface.

The wavelength of the buckling patterns was measured using a custom-designed small-angle light scattering (SALS) apparatus equipped with a computer-controlled $x-y$ translation stage. The translation stage enables rastering of the sample across the laser beam, transforming the SALS apparatus into a high-throughput measurement platform. The scattering patterns were calibrated against a 2500 lpi Ronchi ruling (Edmund Optics, Barrington, NJ) and quantified using an Interactive Data Language (IDL) program to measure the distance between the scattering peaks. Modulus values determined via buckling are the average of >20 scattering patterns per specimen and two specimens per formulation.

Optical images were collected on a Nikon Optiphot microscope equipped with a Kodak ES 1.0 CCD camera. The microscope is outfitted with a Ludl BioPrecision automated stage for acquiring images as a function of spatial position across the sample. The buckling wavelength was calculated from optical images by applying a Fourier transform and determining the dominant wavelength.

The PS/poly(HEMA) specimens were prepared using a slightly different procedure because the hydrogel surfaces are not as adhesive as the PDMS samples. As a result, the PS films had to be floated onto the hydrogel surfaces. This was achieved by gently dipping the PS-coated silicon wafer specimens into a distilled water bath to transfer the PS film onto the surface of the water. The rectangular hydrogel specimen was positioned under the floating PS film and gently raised out of the water, thus transferring the film to the surface of the hydrogel. After allowing a few moments for the surfaces to dry and the film to adhere to the hydrogel surface, the specimens were clamped into a vice and partially resubmerged

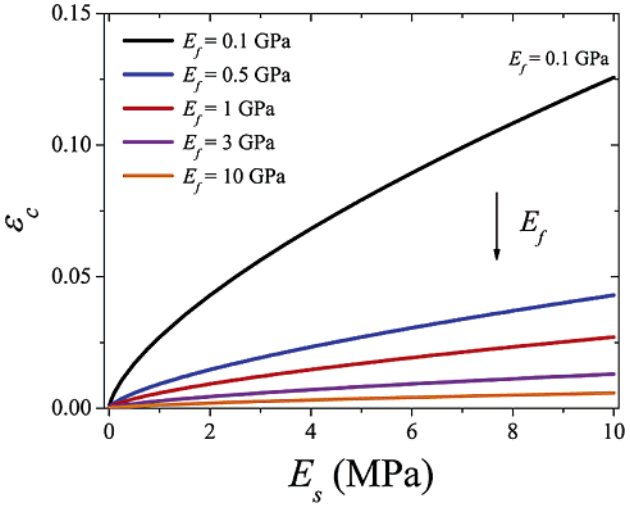

Figure 2. Dependence of the critical strain (ϵ_c) to induce buckling on the substrate modulus (E_s) for a relevant range of sensor film moduli (E_f).

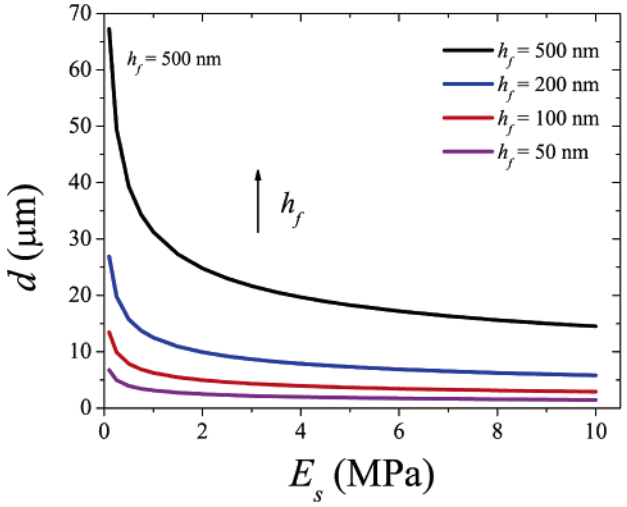

Figure 3. Predicted sensitivity of buckling wavelength (d) on the substrate modulus (E_s) as a function of sensor film thickness (h). The modulus of the sensor film (E_f) is taken as 3.5 GPa, the measured value for PS.[16]

in water to limit evaporation, and a small compression was applied to induce buckling. The buckling patterns were measured by optical microscopy in the same fashion as the PDMS specimens.

Validation Tests. The results obtained from the buckling experiments were validated against bulk mechanical tests. For the PDMS substrates, the Young's moduli were obtained using a texture analyzer (model TA.XT2i, Texture Technologies Corp., Scarsdale, NY) in tension mode. Samples were strained from 50 to 52.50 mm (i.e., 5%) at a rate of 0.1 mm/s. The slope of the stress vs strain curve over the range of 0−2% strain was used to calculate the modulus. One repeat measurement was performed on each specimen for a total of two tensile tests per specimen. The reported results are the average of the four specimens used in the buckling tests plus two additional specimens that had not been previously used.

To validate the results of the hydrogel studies, compression tests were performed on a RSA III dynamic mechanical analyzer (TA Instruments, New Castle, DE). Hydrogel specimens (diameter ≈ 8 mm, height ≈ 5 mm) were placed between parallel plates, and a compressive force was applied at a rate of 0.05 mm/s. Data over the range of 0−5% strain were used to determine an elastic modulus. A minimum of five samples were used in the uniaxial compression testing.

Results and Discussion

Before employing the buckling metrology for determining the soft substrate modulus, the first step is to gauge the sensitivity of this metrology to the governing factors such as critical strain, sensor film thickness and modulus, and substrate modulus in ranges anticipated for polymeric gels and soft networks.

The critical strain (ϵ_c) needed to induce buckling is[20]

$$\epsilon_c = -\frac{1}{4}\left(\frac{3\bar{E}_s}{\bar{E}_f}\right)^{2/3} \tag{5}$$

Figure 2 plots the theoretical dependence of the critical strain (ϵ_c) for buckling on the substrate modulus (E_s) based on eq 5 for a relevant range of sensor film moduli (E_f). The critical strain should be minimal so that the material responses remain in the linear-elastic regime. Moreover, application of sufficiently high strains to the sensor film could lead to crazing, fracture, yielding, or delamination. For all substrate moduli, the critical strain increases dramatically as the sensor film modulus decreases. Thus, Figure 2 demonstrates that the sensor film should be at least a few orders of magnitude greater in modulus than the substrate in order to minimize the critical strain for buckling. To satisfy this criterion, PS (E_f = 3.5 GPa) was chosen as the sensor film since it transfers easily from silicon wafers to PDMS and has a well-characterized modulus.[16]

Likewise, the sensitivity of the buckling wavelength (d) to the substrate modulus (E_s) can be calculated through eq 1. Figure 3 plots the predicted wavelength as a function of substrate modulus for the same PS sensor film over a range of film thickness. As a point of reference, the experimental uncertainty in measuring the buckling wavelength using the SALS apparatus is ± 0.2 μm. Results from Figure 3 demonstrate that thicker films (h > 100 nm) provide greater measurement sensitivity for d over the range of substrate modulus of interest (E_s < 10 MPa), whereas thinner films (h < 50 nm) provide less variation in d over the same range of substrate modulus. On the other hand, thicker films are more prone to delamination from the substrate due to the increased stiffness. Therefore, it is prudent to use a sensor film of intermediate thickness in order to balance sensitivity against adhesion. In the current experiments, we chose a sensor film having a thickness of ~100 nm.

Additionally, the buckling wavelength will also dictate the smallest specimen that can be measured with this technique. There exists a singularity at the edges of the sample where the stress becomes zero (σ_x = 0). The stress distribution away from the free edge can be described analytically[23] by the following equations:

$$\sigma_x = -\sigma_0(1 - e^{-|x|/l}) \tag{6}$$

where l is the characteristic length away from the free edge before the stress becomes constant:

$$l \approx 0.3h_f\left(\frac{\bar{E}_f}{\bar{E}_s}\right) \tag{7}$$

For a PS film (E_f = 3.5 GPa) on a soft substrate (E_s = 1.0 MPa), the characteristic length would be $l \approx 10^3 h_f$. Conversely, this length can be defined in terms of the buckling wavelength through eq 1, which yields a characteristic length of $l \approx 10d$. Consequently, the smallest specimen that would generate a buckling pattern of uniform wavelength and amplitude must have dimensions greater than $2l$ in both x and y. The factor of 2 stems from the fact that there are two free edges at $+x$ and

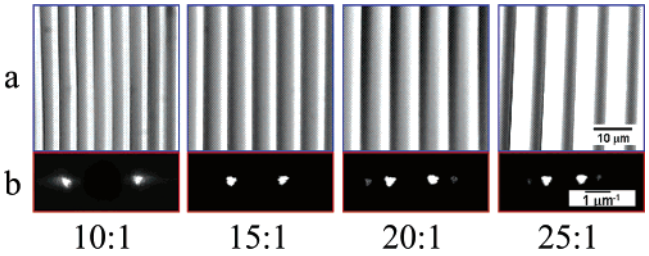

Figure 4. Buckling patterns for a PS sensor film on PDMS with different mass ratios of base to curing agent as viewed by (a) optical microscopy and (b) small-angle light scattering.

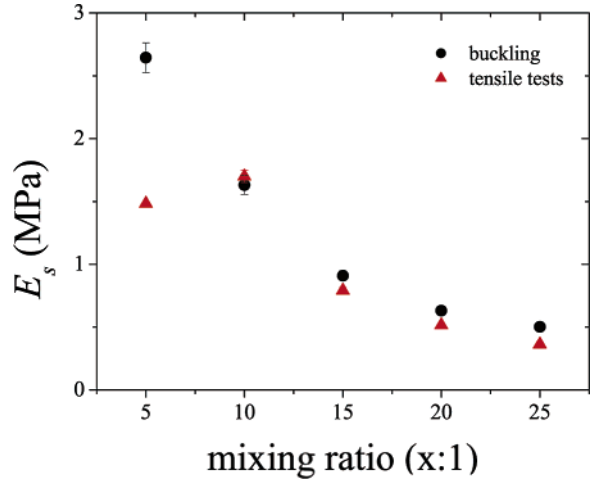

Figure 5. Modulus (E_s) of PDMS elastomers as probed by buckling (●) and traditional tensile tests (▲). The sensor film is PS. The error bars represent one standard deviation of the data, which is taken as the experimental uncertainty of the measurement. Most error bars are smaller than the symbols.

$-x$ coordinates. It would be prudent to sample at least 10 waves to accurately ascribe an average wavelength, hence making the smallest specimen dimensions 30d. For the example given above ($h_f = 100$ nm PS on a 1.0 MPa substrate), the smallest specimen would be ~300 μm. This illustrates one of the advantages of this technique.

To establish this approach as a method to quantify the modulus of soft polymer networks, PDMS was selected as a model substrate since it approximates an ideal elastomer. In addition, PDMS is optically transparent, and its modulus can be tuned by adjusting the mass fraction of base monomer to curing agent in the precured formulation. For these buckling experiments, the PS was applied to PDMS substrates that had been prestrained. Upon release of the strain, a net compressive strain is applied to the PS/PDMS bilayer and the specimen buckles. The buckling wavelength can be determined by either optical microscopy or light scattering, as shown in Figure 4. As the mass fraction of base monomer to curing agent increases, the anticipated substrate modulus decreases (e.g., lower cross-link density). Thus, the buckling wavelength should increase as the substrate provides less resistance to elastic deformation in the z-axis. This is indeed what is observed in Figure 4. The substrate moduli were quantified through eq 3 using the wavelengths of the buckling patterns as determined via SALS. For these samples, SALS is preferred over optical microscopy since there is no need to focus on the surface, lending itself to high-throughput data acquisition, and image processing is more straightforward. The results from the model PDMS elastomer system are shown in Figure 5. The Poisson's ratio for PDMS was taken as $\nu_s = 0.5$. For comparison, the moduli of the PDMS elastomers determined by bulk tensile tests are also shown.

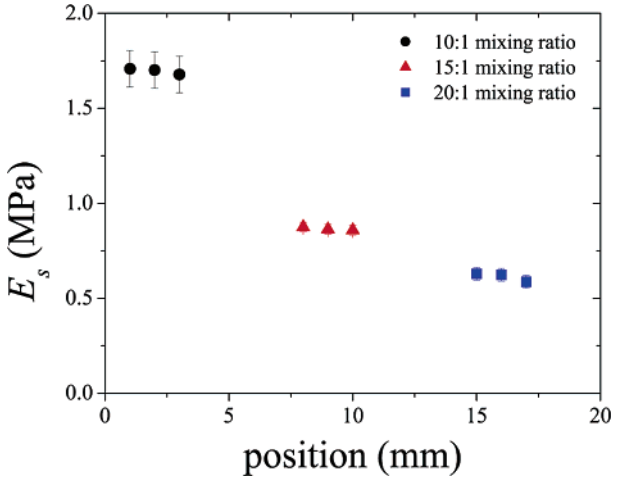

Figure 6. Modulus (E_s) of a PDMS elastomer comprised of a discrete gradient in mixing ratio of base:curing agent in the PDMS formulation as probed by buckling. The sensor film is PS. The error bars represent one standard deviation of the data, which is taken as the experimental uncertainty of the measurement. Most error bars are smaller than the symbols.

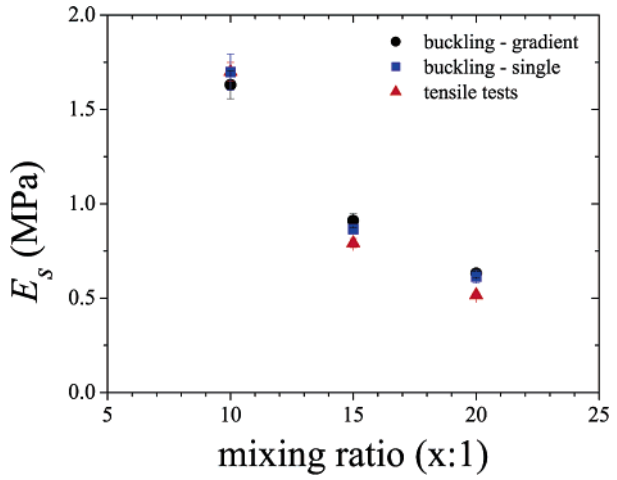

Figure 7. Comparison of modulus data obtained via buckling of a discrete gradient sample (●), buckling of individual single samples (■), and traditional tensile tests (▲) for different mixing ratios of base:curing agent in the PDMS formulation. In the buckling experiments, the sensor film is PS. The error bars represent one standard deviation of the data, which is taken as the experimental uncertainty of the measurement. Most error bars are smaller than the symbols.

There is excellent agreement between the moduli as calculated from the buckling metrology and tensile tests. The exception is the 5:1 mixing ratio, where there is a large, reproducible discrepancy between the results obtained by the two techniques. The cause of the disagreement is unknown at this time; however, the modulus calculated from buckling follows the trend of increasing modulus with decreasing mixing ratio. On the other hand, it is unclear what happens when Sylgard 184 is mixed off the stoichiometry prescribed by the manufacturer (10:1). At low mixing ratios, there will be an excess of cross-linker in the system, which could lead to a plateau in modulus below a 10:1 mixing ratio. There is, on average, a disparity of 0.1 MPa between the buckling and tensile test data, which serves as an indication of the accuracy of the measurement.

The main advantage for the buckling metrology is its ability to rapidly characterize substrates that have nonuniform moduli. This concept is tested on a PDMS modulus gradient sample comprised of three discrete steps in base monomer to curing agent ratios. The discrete steps were perpendicular to the strain

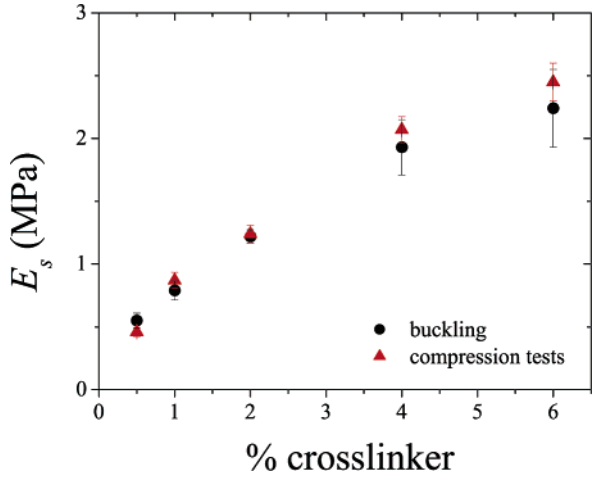

Figure 8. Modulus (E_s) of poly(HEMA) hydrogels as probed by buckling (●) and traditional compression tests (▲) as a function of cross-linker mass fraction in the hydrogel formulation. The sensor film is PS. The error bars represent one standard deviation of the data, which is taken as the experimental uncertainty of the measurement. Most error bars are smaller than the symbols.

direction, thus ensuring that each section will be subjected to identical strains. The same compositions used in the gradient sample preparation were cast as individual samples for validation against uniform buckling tests as well as traditional tensile tests. The buckling wavelength was again ascertained by SALS. Figure 6 displays the substrate modulus as a function of spatial position across the gradient PDMS substrate. In these experiments, the buckling wavelength varied spatially across the specimen, and the resulting modulus depended on the specific mixing ratio under the film. The error bars are generated by calculating the standard deviation of the data along a single column of diffraction patterns, whereas each row corresponds to different positions across the sample. Figure 7 shows moduli obtained from the buckling of individual samples and the gradient sample as well as bulk tensile tests. The moduli calculated from buckling of the gradient specimen and individual specimens compare well to each other, while the modulus obtained from tensile tests are again lower by ≈0.1 MPa. Indeed, these results demonstrate that a modulus map can be generated across the gradient specimen with the buckling metrology. This type of modulus mapping cannot be done with conventional tensile tests since the specimen would act as a composite material.

To extend the applicability of the buckling metrology as well as demonstrate its versatility, we investigate its use for determining the modulus of commonly used and commercially relevant poly(HEMA) hydrogels. As mentioned previously, the adhesion between PS and a poly(HEMA) hydrogel is not as favorable as that between PS and PDMS; therefore, a modified experimental protocol is necessary to assemble the film/substrate bilayer, as described in the Experimental Section. In addition, the poly(HEMA) hydrogels we prepared are not fully transparent, particular those with less cross-linker, rendering optical microscopy the more appropriate characterization technique. Figure 8 illustrates the hydrogel moduli determined using the buckling metrology as compared to uniaxial compression testing. The Poisson's ratio of the hydrogels was taken as $\nu_s = 0.5$. As expected, the modulus of the poly(HEMA) hydrogels increases with increasing cross-linker content. Excellent agreement in moduli is found between buckling and compression tests for all cross-linker compositions. However, the standard uncertainty for the buckling metrology increases as the substrate modulus is increased, and this is attributed to the diminished sensitivity with increasing substrate modulus (Figure 3) and is augmented by uncertainties inherent to the optical microscope (for a constant magnification) as the buckling wavelength decreases. Nevertheless, these results indicate that the buckling metrology is an effective approach for determining the modulus of soft hydrogels.

The strength of the buckling metrology resides in its ability to characterize localized properties. This would be particularly useful for samples having nonuniform geometries and/or properties. To illustrate this, the moduli of a gradient specimen consisting of HEMA polymerized with different cross-linker compositions were determined with the buckling metrology. In these experiments, the thickness of the PS sensor film was $h_f = 98 \pm 2$ nm. Figure 9 shows representative optical micrographs of buckling patterns taken across the poly(HEMA) gradient specimen. Five zones are clearly visible. The wavelength decreases as the cross-linker content increases, indicating that the modulus increases as the cross-linker content is increased. In some areas, artifacts unrelated to the buckling pattern are

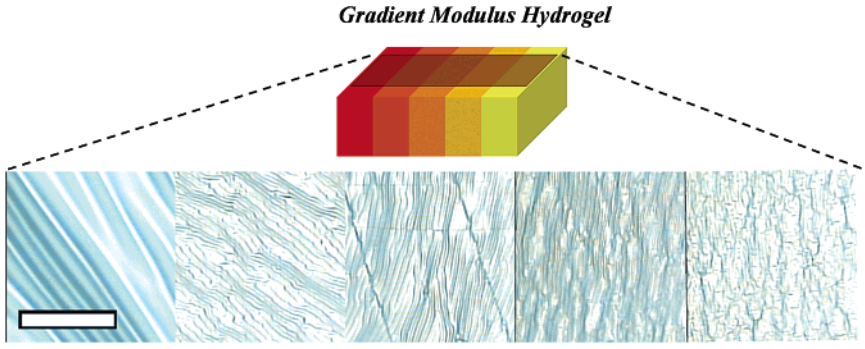

Zone	1	2	3	4	5
Cross-linker	0.5 %	1 %	2 %	4 %	8 %
E_s (MPa)	0.56 MPa	0.81 MPa	1.2 MPa	2.0 MPa	2.6 MPa
σ (MPa)	± 0.06 MPa	± 0.07 MPa	± 0.06 MPa	± 0.43 MPa	± 0.51 MPa

Figure 9. (top) Optical microscopy of buckling patterns for a PS sensor film on poly(HEMA) hydrogels comprised of a discrete gradient in the mass fraction of cross-linker in the hydrogel formulation. The scale bar in the optical images is 100 μm. (bottom) The table shows the cross-linker content and corresponding modulus (E_s) and standard deviation (σ) for each zone of the discrete gradient.

observed, particularly for compositions high in the cross-linker content. In addition, the buckling patterns become more isotropic in these samples due to slight deswelling of the hydrogels, which generates an isotropic component to the overall applied strain. Moreover, cracks perpendicular to the buckling pattern are visible for the 8% cross-linker poly(HEMA) hydrogels. It should be noted that these imperfections do not impinge on the modulus calculation. The corresponding modulus calculated from those buckling patterns (listed in Figure 9) are consistent with those obtained by traditional compression tests as well as single buckling specimens. Overall, results from the gradient specimen demonstrate that modulus maps can be generated using the current buckling metrology.

Conclusions

We employ buckling of a sensor film applied to soft polymer networks to report back the elastic modulus of the network phase. The metrology was demonstrated on a model system comprised of PDMS with varying cross-link density, where the buckling wavelength could be determined by small-angle light scattering due to the optical transparency of the PDMS. The metrology was then applied to a commercially relevant system consisting of cross-linked poly(HEMA) hydrogels. In this system, optical microscopy was employed to determine the buckling wavelength due to the propensity of the hydrogel networks to be slightly opaque at lower cross-linker concentrations. In all cases, excellent agreement between the buckling metrology and conventional tensile or compression tests was observed. Moreover, we show how this metrology can be used to map spatial differences in modulus over a specimen by using graded substrates for both the model PDMS system and the poly(HEMA) hydrogel system. Indeed, the ability to spatially map the modulus across a gradient specimen is a distinguishing feature of this metrology, which cannot be accomplished with conventional methods for measuring elastic modulus.

Acknowledgment. The resins and initiator were kindly donated by Esstech, Inc. and Ciba Specialty Chemical Corp., respectively. E.A.W. acknowledges the NIST/NRC Postdoctoral Fellowship Program for funding. In addition, the authors thank Drs. Joseph M. Antonucci and Martin Y. M. Chiang for their advice and technical recommendations.

References and Notes

(1) Bryant, S. J.; Anseth, K. S. *J. Biomed. Mater. Res.* **2002**, *59*, 63−72.
(2) Kim, U. J.; Park, J. H.; Li, C. M.; Jin, H. J.; Valluzzi, R.; Kaplan, D. L. *Biomacromolecules* **2005**, *5*, 786−792.
(3) Almany, L.; Seliktar, D. *Biomaterials* **2005**, *26*, 2467−2477.
(4) Anseth, K. S.; Bowman, C. N.; Brannon-Peppas, L. *Biomaterials* **1996**, *17*, 1647−1657.
(5) Thompson, M. T.; Berg, M. C.; Tobias, I. S.; Rubner, M. F.; Van Vliet, K. J. *Biomaterials* **2005**, *26*, 6836−6845.
(6) Mei, Y.; Beers, K. L.; Byrd, H. C. M.; VanderHart, D. L.; Washburn, N. R. *J. Am. Chem. Soc.* **2004**, *126*, 3472−3476.
(7) Schneider, J. P.; Pochan, D. J.; Ozbas, B.; Rajagopal, K.; Pakstis, L.; Kretsinger, J. *J. Am. Chem. Soc.* **2002**, *124*, 15030−15037.
(8) Kim, U. J.; Park, J. Y.; Li, C. M.; Jin, H. J.; Valluzzi, R.; Kaplan, D. L. *Biomacromolecules* **2004**, *5*, 786−792.
(9) Iwasaki, Y.; Nakagawa, C.; Ohtomi, M.; Ishihara, K.; Akiyoshi, K. *Biomacromolecules* **2004**, *5*, 1110−1115.
(10) Rolland, J. P.; Van Dam, R. M.; Schorzman, D. A.; Quake, S. R.; DeSimone, J. M. *J. Am. Chem. Soc.* **2004**, *126*, 2322−2323.
(11) Andre, S.; Guida-Pietrasanta, F.; Rousseau, A.; Boutevin, B.; Caporiccio, G. *J. Polym. Sci., Part B: Polym. Phys.* **2004**, *42*, 200−207.
(12) Bai, S.; Zhao, Y. *Macromolecules* **2001**, *34*, 9032−9038.
(13) Oliver, W. C.; Pharr, G. M. *J. Mater. Res.* **2004**, *19*, 3−20.
(14) VanLandingham, M. R. *J. Res. Natl. Inst. Stand. Technol.* **2003**, *108*, 249−265.
(15) VanLandingham, M. R.; Villarrubia, J. S.; Guthrie, W. F.; Meyers, G. F. *Macromol. Symp.* **2001**, *167*, 15−43.
(16) Stafford, C. M.; Harrison, C.; Beers, K. L.; Karim, A.; Amis, E. J.; VanLandingham, M. R.; Kim, H. C.; Volksen, W.; Miller, R. D.; Simonyi, E. E. *Nat. Mater.* **2004**, *3*, 545−550.
(17) Stafford, C. M.; Guo, S.; Harrison, C.; Chiang, M. Y. M. *Rev. Sci. Insrum.* **2005**, *76*, 062207.
(18) Gough, G. S.; Elam, C. F.; de Bruyne, N. A. *J. R. Aeronaut. Soc.* **1940**, *44*, 12.
(19) Allen, H. G. *Analysis and Design of Structural Sandwich Panels*; Pergamon: New York, 1969.
(20) Groenewold, J. *Physica A* **2001**, *298*, 32−45.
(21) Huang, Z. Y.; Hong, W.; Suo, Z. *J. Mech. Phys. Solids* **2005**, *53*, 2101−2118.
(22) Certain equipment, instruments or materials are identified in this paper in order to adequately specify the experimental details. Such identification does not imply recommendation by the National Institute of Standards and Technology nor does it imply the materials are necessarily the best available for the purpose.
(23) Bowden, N.; Brittain, S.; Evans, A. G.; Hutchinson, J. W.; Whitesides, G. M. *Nature (London)* **1998**, *393*, 146−149.

MA060266B